Improved Clearance during Treatment of HPV-Positive Head and Neck Cancer through mTOR Inhibition[1,2]

Joseph D. Coppock[*], Bryant G. Wieking[*], Alfredo A. Molinolo[†], J. Silvio Gutkind[†], W. Keith Miskimins[*] and John H. Lee[*,‡]

[*]Cancer Biology Research Center, Sanford Research/USD, Sioux Falls, SD; [†]Oral and Pharyngeal Cancer Branch, National Institute of Dental and Craniofacial Research, National Institutes of Health, Bethesda, MD; [‡]Department of Otolaryngology/Head and Neck Surgery, Sanford Health, Sioux Falls, SD

Abstract

Human papillomavirus (HPV)–related head and neck squamous cell carcinoma (HNSCC) incidence is increasing at a near epidemic rate. We investigated whether the mammalian (or mechanistic) target of rapamycin (mTOR) inhibitor, rapamycin, can be used as a concurrent agent to standard-of-care cisplatin/radiation therapy (CRT) to attenuate tumor lactate production, thus enhancing CRT-induced immune-mediated clearance of this antigenic tumor type. A C57Bl/6-derived mouse oropharyngeal epithelial cell line retrovirally transduced with HPV type 16 E6/E7 and human squamous cell carcinoma cell lines were evaluated for their response to rapamycin *in vitro* with proliferation assays, Western blots, and lactate assays. Clonogenic assays and a preclinical mouse model were used to assess rapamycin as a concurrent agent to CRT. The potential of rapamycin to enhance immune response through lactate attenuation was assessed using quantitative tumor lactate bioluminescence and assessment of cell-mediated immunity using E6/E7-vaccinated mouse splenocytes. Rapamycin alone inhibited mTOR signaling of all cancer cell lines tested *in vitro* and *in vivo*. Furthermore, rapamycin administered alone significantly prolonged survival *in vivo* but did not result in any long-term cures. Given concurrently, CRT/rapamycin significantly enhanced direct cell killing in clonogenic assays and prolonged survival in immunocompromised mice. However, in immunocompetent mice, concurrent CRT/rapamycin increased long-term cures by 21%. Preliminary findings suggest that improved survival involves increased cell killing and enhanced immune-mediated clearance in part due to decreased lactate production. The results may provide rationale for the clinical evaluation of mTOR inhibitors concurrent with standard-of-care CRT for treatment of HPV-positive HNSCC.

Neoplasia (2013) 15, 620–630

Introduction

Three to five percent of all cancers reported in the United States are head and neck squamous cell carcinomas (HNSCCs), with more than 40,000 cases reported annually [1]. Survival rates for this type of cancer are poor. Only about 50% of patients will survive over the 5-year period following diagnosis. Though incidence of head and neck cancer is on a general decline, correlating with decreasing smoking prevalence [2], human papillomavirus (HPV)–related HNSCC is increasing at a near epidemic rate with incidence nearly tripling over the last 30 years [3,4]. Of the more than 40,000 reported annual cases of HNSCC in the United States, at least 25% are HPV type 16 (HPV-16) positive and roughly 40% result in death [5–7]. More specifically, an even greater proportion (60–80%) of *oropharyngeal* HNSCC is HPV-16 positive (HPV+). These tumors present with more advanced stage disease compared to their histologically identical HPV-negative (HPV–) counterparts [5,6,8]. Though more advanced, HPV+ tumors paradoxically leave patients with an improved prognosis with standard-of-care combined modality treatment, which typically includes surgery, cisplatin, and radiation. The improved prognosis is likely imparted by the antigenic nature of this tumor type [2,9], though it has also been attributed to maintenance of functional unmutated p53 [5]. While HPV+ HNSCCs have an improved survival compared to HPV– counterparts, the increasing incidence makes understanding this disease a priority. Although successful in at least 80% of patients, treatments also leave patients with significant morbidity associated with eating and speaking. Together, increasing disease burden and significant treatment-related morbidity necessitate the need to develop better therapies or dose-reducing adjuvants.

One of the key cancer characteristics that contribute to the poor prognosis of HNSCC is altered cellular metabolism. Unlike normal cells, which generate energy through oxidative phosphorylation, cancer cells use high rates of glycolysis to generate cellular energy and produce biosynthetic intermediates. This allows them to live in low- and fluctuating oxygen environments [10]. Normal cells use oxidative phosphorylation through the tricarboxylic acid cycle and electron transport chain, fermenting only under hypoxic conditions when the greater energy producing tricarboxylic acid–electron transport chain pathway cannot be used. Cancer cells, however, alter key metabolic enzymes that allow them to thrive in low-oxygen environments. This phenomenon is known as the Warburg effect, or aerobic glycolysis, in which cancer cells use glycolysis and fermentation of pyruvate into lactate as a primary energy pathway even in the presence of sufficient oxygen [11].

The most common subset of hypermetabolic HNSCC is that caused by HPV [12]. Expression of the HPV E6 oncoprotein causes p53 degradation, and this is required for malignant transformation by the virus. Although not fully understood, HPV oncogenes play a role in conferring the metabolic phenotype of related HNSCC. Recent evidence has suggested that the E6 oncoprotein also alters cellular metabolism [13]. The E6 oncoprotein has been shown to promote a highly metabolic phenotype through increases in mammalian (or mechanistic) target of rapamycin (mTOR) activity [14]. mTOR activity is upregulated in head and neck cancers and plays a critical role in controlling factors that impact local recurrence and survival in HNSCC, including metabolism [15–17]. Specifically, mTOR increases expression of hypoxia-inducible factor 1α (HIF1α) and subsequently pyruvate kinase M2, lactate dehydrogenase (LDH), pyruvate dehydrogenase kinase 1, and GLUT1, among other proteins regulated by the hypoxia response element [18,19]. Through these pathways, E6 activation of mTOR plays a role in altering cellular metabolic function.

The mTOR inhibitor, rapamycin (sirolimus), is commonly used in combination with glucocorticoids and cyclosporine to prevent organ rejection. Even at these synergistic, immunosuppressive doses, it is well tolerated and has minimal toxicity [15,16], making it an attractive adjuvant along with already being approved for use in human patients. Used alone, rapamycin does not cause significant immune suppression but instead has been shown to prevent progression, slow growth, and impede angiogenesis and lymphangiogenesis in various tumor models, including head and neck [20–24]. The reliance of head and neck cancers on the mTOR signaling pathway has led to increased interest in using rapamycin as a head and neck cancer treatment specifically [15,16].

We have recently shown that an immune response is required for long-term cures of HPV+ HNSCC following standard cisplatin/radiation therapy (CRT) [9] and that this immune-mediated clearance is CD8+ dependent [25]. While activated mTOR signaling promotes lactate production as a byproduct of upregulated metabolism, lactate in the tumor microenvironment has been shown to inhibit immune cell functions [26–28], including those specific for CD8+ cells [29]. We thus hypothesized that appropriately inhibiting tumor metabolism through inhibition of mTOR may improve survival by at least two mechanisms: 1) enhanced direct cell toxicity due to blocking of key survival signals and 2) attenuation of tumor lactate production that could enhance immune-mediated tumor clearance. To investigate this hypothesis, we examined how inhibition of mTOR signaling by rapamycin alone affects growth and how it synergizes with CRT to potentially enhance therapeutic efficacy. Though classified as an immunosuppressant, indeed rapamycin has also been shown to have particular immune-enhancing capabilities ([30,31] and references therein). Here, we show that mTOR inhibition by rapamycin, along with the consequent reduction of lactate levels, may be a relatively safe, nontoxic way to both enhance direct CRT-induced cytotoxicity and the tumor clearing immune response to HPV+ HNSCC.

Materials and Methods

Cell Lines, Culture Conditions, and Authentication

Mouse oropharyngeal epithelial cells (MOEs) were previously internally derived from C57Bl/6 mouse oropharyngeal epithelium retrovirally transduced with the indicated vectors and oncogenes [7]. MOEs are routinely internally screened for the presence of cytokeratin and HPV-16 mRNA as means of authentication, and our model HPV+ HNSCC line harboring the *E6*, *E7*, and mutated *H-Ras*^{V12} oncogenes (E6/E7/Ras MOEs) [32] is routinely grafted into syngeneic mice for animal studies. Human squamous cell carcinoma cell (SCC) lines 1, 47, and 84 were a generous gift from Dr Douglas Trask (University of Iowa, Iowa City, IA). These human cell lines were originally generated at the University of Michigan (UM-SCCs; Ann Arbor, MI) by the Head and Neck SPORE Translational Research Group. This group has completed genotyping of 73 published UM-SCC cell lines [33]. Results from continued efforts to genotype remaining and newly generated cell lines are posted on the UM Head and Neck SPORE Tissue Core web site (http://www2.med.umich.edu/cancer/hnspore/cores-tissue.cfm). The UM-SCC cell lines used in this work were authenticated by Genetica DNA Laboratories (Cincinnati, OH) through DNA profiling and are also routinely internally screened for HPV-16 mRNA. The SCC90 cell line was a gift during the period of this work from Dr Randall Kimple (University of Wisconsin, Madison, WI) who received it directly from the University of Pittsburgh (UP-SCC90). MOEs and SCCs were maintained in Dulbecco's modified Eagle's

medium (Hyclone, Logan, UT) supplemented with 10% FBS (Atlanta Biologicals, Lawrenceville, GA), 100 U/ml penicillin (Hyclone), 100 µg/ml streptomycin (Hyclone), and 250 ng/ml amphotericin B (CellGro, Manassas, VA). Primary human tonsil epithelial cells (HTEs) were internally cultured from normal human tonsil epithelium, and experiments were performed within three passages. Primary HTEs were cultured in keratinocyte serum-free media supplemented with 0.025 mg/ml bovine pituitary extract (Gibco, Grand Island, NY) and 1.6×10^{-4} µg/ml epidermal growth factor (Gibco). All cells were cultured at 37°C in a 5% CO_2 humidified atmosphere.

Cell Proliferation and Lactate Assays

Cell lines were plated in triplicate and allowed to establish for 24 hours before treating with the indicated concentrations of rapamycin (LC Laboratories, Woburn, MA) dissolved in DMSO in culture media. After 72 hours, all cells were isolated, resuspended, and stained 1:1 with 0.4% trypan blue (Sigma-Aldrich, St Louis, MO). Live and dead cell numbers were counted through a hemacytometer with live cell number presented as percent of control live cell number. Lactate levels in the culture media were determined using colorimetric enzymatic assays. Cells were plated in triplicate and allowed to grow to 100% confluence before treating with the indicated concentrations of rapamycin for 4 hours. Culture media was then subject to the standard protocol of a commercially available lactate assay kit (Eton Bioscience, San Diego, CA). Absorbance (A490) was read on a SpectraMax Plus 384 plate reader, and a standard curve was generated for back-calculation of lactate concentration.

Clonogenic Assays

Cells were plated in triplicate at 2500 E6/E7/Ras MOEs per 100-mm dish for each of the indicated rapamycin concentrations. Cells were allowed to establish for 24 hours before beginning a 1-day pretreatment of rapamycin, mimicking our *in vivo* treatment regimen. Media containing both the indicated concentration of rapamycin and 0.5 µg/ml cisplatin (Calbiochem, Darmstadt, Germany) dissolved in normal saline were then replaced. After a 1-hour incubation, all cells were irradiated (4 Gy) and returned to the incubator. A week from the initiation of treatment, cells were fixed in 70% ethanol and stained with 0.5% crystal violet (Fisher, Waltham, MA) in 10% ethanol. Average size and number of colonies, defined as a minimum of 50 cells, were quantified using an AlphaImager System and corresponding image analysis software (AlphaInnotech, Santa Clara, CA).

Western Blot Analysis of the mTOR Pathway

Cells were harvested in a sodium dodecyl sulfate (SDS)–containing buffer [2.5 mM Tris-HCl (pH 6.8), 2.5% SDS, 100 mM DTT, 10% glycerol, and 0.025% pyronine Y] at 24 hours, sonicated, and heated before running. Equal amounts of protein were separated by SDS–polyacrylamide gel electrophoresis and transferred to polyvinylidene difluoride (PVDF) membrane through semidry transfer apparatus. Antibodies for detection of proteins of interest were diluted in blocking buffer, 5% BSA or nonfat dry milk in tris-buffered saline with tween (TBST), as recommended for individual antibodies: phosphorylated p70 S6 kinase (P-S6K; Thr389, #9206; Cell Signaling Technology, Danvers, MA), p70 S6K (#9202; Cell Signaling Technology), 4E-BP1 (R-113, sc-6936; Santa Cruz Biotechnology, Santa Cruz, CA). Signal was detected using HRP-conjugated secondary antibodies and Amersham ECL prime detection reagent (GE Healthcare, Little Chalfont, United

Kingdom). Exposures were captured using a charged-coupled device (CCD) camera imaging system (UVP, Upland, CA).

Animal Studies

Our *in vivo* model of HPV+ HNSCC was used as described previously [9]. All experiments were performed in accordance with institutional and national guidelines and regulations with the protocol approved by the Animal Care and Use Committee at Sanford Research. Briefly, 1×10^6 E6/E7/Ras MOEs were injected into the right subcutaneous flank of syngeneic male C57Bl/6 mice (immune competent) or B6.129S7-$Rag1^{tm1Mom}$/J (RAG-1 or Rag) mice (immunocompromised, lacking mature B and T cells). Tumors were allowed to establish for 1 to 2 weeks before treatment administration. Mice were administered rapamycin intraperitoneally (i.p.) in a 5.2% Tween 80 (Sigma-Aldrich), 5.2% PEG-400 (Hampton Research, Aliso Viejo, CA) phosphate-buffered saline vehicle at 0 to 5.0 mg/kg as previously described [22]. Rapamycin or vehicle was administered daily to end point or for 21 days when concurrent with 3 weeks of once weekly i.p. cisplatin (0.132 mg/mouse) dissolved in normal saline and once weekly radiation (8 Gy; 24 Gy total) to the affected flank. Tumor dimensions were measured weekly to monitor growth. Mice with tumors obtaining a volume of 3000 mm^3 or becoming substantially emaciated were euthanized. When all mice reached end point or a maximum of 100 days passed, Kaplan-Meier survival analysis was performed on the basis of exponential regressions of individual tumor volume curves, standardizing survival to the predefined 3000-mm^3 tumor volume end point.

Tumor Immunohistochemistry and Lactate Bioluminescence

Anti–phospho-S6 (Ser235/236, #2211S; Cell Signaling Technology) was used for immunohistochemical analysis of paraffin-embedded tumors harvested from daily rapamycin- or vehicle-treated mice at end point as previously described [22]. Stained slides were scanned with an Aperio CS Scanscope. Quantitative tumor lactate bioluminescence was performed as recently described by Broggini-Tenzer et al. [34]. Twenty-micrometer sections of tumors as described above, flash-frozen in freezing media optimal cutting temperature (OCT), were heat inactivated (100°C) on standard microscope slides. Fifty microliters of lactate-dependent luciferase-containing buffer was added to each tumor section followed by immediate imaging on a Carestream In Vivo Xtreme Small Animal Imaging System. Average intensities of each section were determined using the provided Carestream software.

Cell-mediated Immunity Assay

Carboxyfluorescein succinimidyl ester (CFSE; Invitrogen, Grand Island, NY)–stained E6/E7/Ras cells were irradiated (30 Gy) and co-cultured 1:10 (target/effector) for 24 hours with isolated mixed lymphocytes from the spleens of mice intranasally vaccinated with a previously developed adenoviral recombinant vaccine expressing HPV-16 E6 and E7 (adenovirus 5 E6/E7, or Ad5 E6/E7) [6] at the indicated concentrations of lactic acid (Sigma-Aldrich) in media (RPMI, supplemented as Dulbecco's modified Eagle's medium above; Hyclone) followed by dead cell staining (TO-PRO-3; Invitrogen) and flow cytometry. Using an Accuri C6 Flow Cytometer and CFlow Plus software (BD-Accuri, Ann Arbor, MI), CFSE-positive cells were gated using the FL2 channel and mean TO-PRO-3 signal averaged for each dosage group using the FL4 channel. Isolated lymphocytes, as described above, were also cultured alone for detection of levels of intracellular perforin. The cells were cultured at the indicated concentrations of lactic acid in media at a cell density of 2.5×10^6 cells/ml for 24 hours, followed by

pelleting and lysing in an SDS-containing buffer for Western blot, as described above. Perforin antibody (#3693; Cell Signaling Technology) was diluted in 5% BSA in TBST as recommended for detection by Western blot.

Statistical Analysis

Error bars displayed are SDs from the mean of at least three replicates. Comparison of two groups was done using two-tailed pairwise Student's t tests. Regarding Kaplan-Meier survival analysis, log-rank significance tests were performed with P values generated using the pairwise multiple comparisons Holm-Sidak method. P values less than or equal to .05 were considered to have significance.

Results

Rapamycin Inhibits HPV+ HNSCC Cell Proliferation with Associated Decreases in mTOR Signaling

Activation of mTOR and its modulation by multiple cellular pathways is a common feature of HNSCC. To assess the potential of rapamycin to inhibit this frequently altered pathway in HNSCC, we examined the effects *in vitro* on cell growth and signaling in primary HTEs (1°), two HPV− SCC cell lines (SCC1 and SCC84), and two HPV+ SCC cell lines (SCC47 and SCC90). All of the cells tested were treated with 0 to 100 nM rapamycin for 72 hours and were inhibited in growth in a dose-dependent manner (all lines at 10–100 nM rapamycin, $P \leq .047$ to untreated control), with 1° HTEs appearing the least sensitive to higher doses (Figure 1*A*), though all cell lines were inhibited in mTOR signaling. This was evidenced by decreases in phosphorylated downstream targets p70 S6K (P-S6K) and eukaryotic initiation factor 4E binding protein 1 (4EBP1) seen by Western blot (Figures 1*B* and W1). These findings reflect the increased mTOR dependence of HNSCC [15,35] over normal epithelium, the latter as recently shown for normal oral keratinocytes [36], and suggest that rapamycin has the potential to exploit this mTOR dependence, including the presumably high mTOR dependence imposed by the E6 oncoprotein in HPV+ HNSCC [14].

We extended these findings to our immortalized MOEs harboring either empty vector (LXSN) or HPV-16 E6 and E7 (E6/E7). These cells were also treated with rapamycin at the indicated doses after which cell viability was determined (Figure 1*C*). Both cell lines were inhibited in mTOR signaling (Figures 1*D* and W1) and responsive to rapamycin treatment in a dose-dependent manner. A caveat is that the empty vector control cell line is an immortalized line and may have greater mTOR dependence than primary epithelial cells and thus shows greater sensitivity to rapamycin. To this end, these findings together with those in the human cells support the potential efficacy of rapamycin in HPV+ HNSCC and warranted further studies.
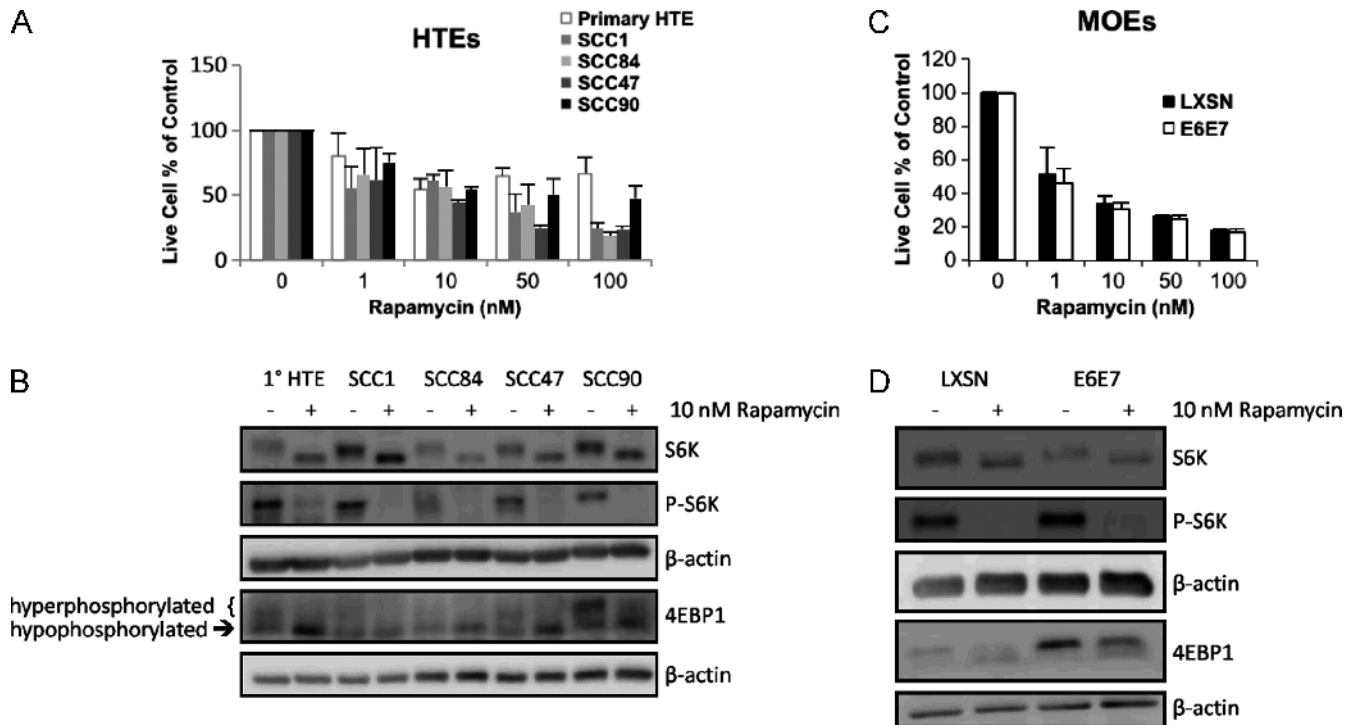

Figure 1. Inhibition of cell proliferation of human and mouse HNSCC cell lines by rapamycin is associated with decreases in mTOR signaling. (A) Cell proliferation assay. Primary HTEs are compared to four tonsillar SCC lines, two HPV− (SCC1 and SCC84) and two HPV+ (SCC47 and SCC90), after 72 hours of rapamycin treatment at the indicated concentrations. (B) Western blot analysis of downstream targets of mTOR. Whole-cell lysates of the cell lines described in A after 24 hours of 10 nM rapamycin treatment were analyzed for protein levels downstream of mTOR. (C) Mouse correlate to A. A retrovirally transduced and immortalized HPV+ mouse oropharyngeal epithelial (MOE) cell line possessing the E6 and E7 oncogenes (E6/E7) is compared to an empty vector containing control line (LXSN). (D) Corresponding mouse correlate Western blots of downstream targets of mTOR. All cell lines treated with rapamycin showed a dose-dependent decrease in cell proliferation (all lines at 10–100 nM rapamycin, $P \leq .047$ to control). Regarding Western blots, with rapamycin treatment, total S6K migrates slightly faster, indicating dephosphorylation. Phosphorylation of S6K (P-S6K) is nearly completely inhibited, and 4EBP1 shows decreases in the slower migrating, hyperphosphorylated bands and increases in the faster migrating, hypophosphorylated bands. Blots have been cropped for presentation and those with dark backgrounds have been enhanced in contrast and brightness in entirety using Microsoft PowerPoint before cropping. Full-length blots can be seen in Figure W1.

Rapamycin Enhances Direct CRT-Induced Cytotoxicity

Many HPV+ cancers are currently treated with concurrent cisplatin and radiation [9,37]. Chemotherapy and radiation are known to activate survival signals through the phosphatidylinositol 3-kinase (PI3K)/Akt/mTOR pathways [38]. Evidence exists for separate radiosensitizing and chemotherapeutic enhancing effects of mTOR inhibition by rapamycin [16,38], and chemotherapy itself is radiosensitizing [15]. However, rapamycin has not been studied extensively in combination with both cisplatin and radiation for HPV+ HNSCC. To assess the ability of rapamycin to enhance the direct cell toxicity of CRT, we used clonogenic assays. Cells were plated 24 hours before a 1-day pretreatment with rapamycin before adding cisplatin and irradiating. In such a manner, we mimicked the treatment regimen used in our animal studies. Dose escalation of rapamycin with stable doses of concurrent cisplatin and radiation resulted in a dose-dependent decrease in colonies formed (1 nM, $P < .03$; 10 nM, $P < .01$) and at significantly smaller sizes ($P < .03$), suggesting that low-dose rapamycin (1–10 nM) significantly enhances direct CRT-induced cytotoxicity (Figure 2). These findings are further supported by our *in vivo* findings that show a statistically significant prolonging of survival in immunocompromised Rag-1–deficient mice when rapamycin was administered concurrently with CRT, as discussed below.
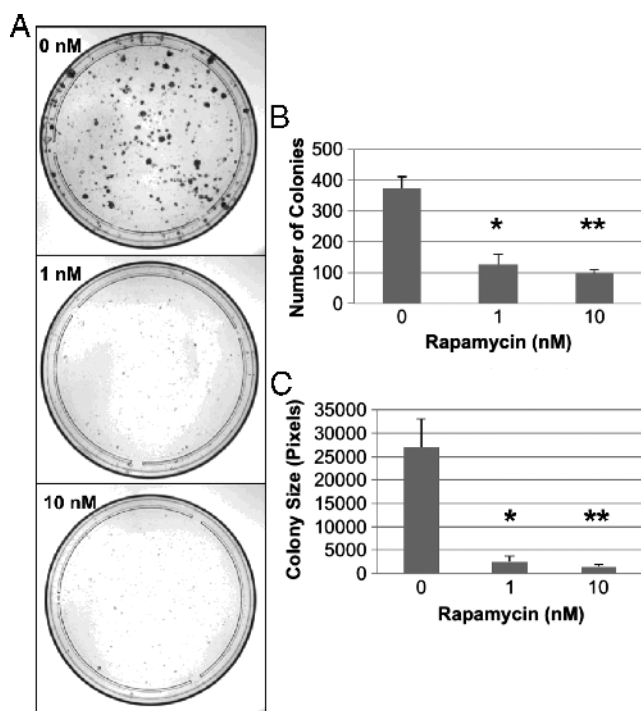

Figure 2. Rapamycin enhances the direct CRT-induced cytotoxicity in clonogenic assays. E6/E7/Ras MOEs allowed to establish for 24 hours were treated with rapamycin at the indicated concentrations for an additional 24 hours. Cells were then dosed with cisplatin and radiation with rapamycin treatment continued concurrently. After 1 week, colonies were fixed, stained, and counted. Representative images of the colonies formed at each rapamycin concentration with equal cisplatin and radiation dosing in all conditions are shown in A. Average colony number at each concentration is shown in B, and average colony size is shown in C. Rapamycin was seen to enhance the direct CRT-induced cytotoxicity to this model HPV+ HNSCC cell line, with fewer (*$P < .03$, **$P < .01$) and smaller (*$P < .03$, **$P < .03$) colonies forming in the presence of rapamycin.

Rapamycin Prolongs Tumor-Bearing Survival and Enhances Immune-Mediated Tumor Clearance

The therapeutic potential of rapamycin was assessed *in vivo* using a previously developed mouse model of HPV+ HNSCC. This model consists of immortalized C57Bl/6 MOEs retrovirally transduced with the HPV-16 *E6* and *E7* oncogenes as well as an activated *H-Ras* gene (E6/E7/Ras cells) injected into the subcutaneous flank of syngeneic mice (as described in greater detail in Materials and Methods section above). Daily rapamycin treatment alone in immunocompetent mice was not sufficient for tumor clearance (Figure 3A), but growth was inhibited enough to the point that tumor-bearing survival time was significantly increased (10.6-day median survival increase by 5 mg/kg rapamycin, $P < .0004$). At the tumor level, immunohistochemical analysis revealed greatly inhibited mTOR signaling through phosphorylated ribosomal S6 staining with rapamycin treatment (Figure 3B). In three separate experiments, when mice were subjected to a 3-week rapamycin regimen concurrent with CRT, rapamycin-treated mice (5 mg/kg) showed a consistent 20% to 30% increase in tumor-free survival to vehicle + CRT–treated mice. The combined overall survival for these three experiments shows a dose-dependent increase in tumor-free survival, with a 21% overall increase ($P \leq .055$) in the highest rapamycin dose + CRT–treated groups compared to vehicle + CRT (Figure 3C). In this wild-type, immunocompetent setting, rapamycin actually increased the number of animals that went on to be tumor-free.

To evaluate the role of the immune system, immunocompromised, Rag-1–deficient C57Bl/6 mice (which lack mature T and B cells [25]) were subjected to the same treatment regimens. Significant increases in tumor-bearing survival were seen with daily rapamycin alone (10 days by 1 mg/kg rapamycin, $P < .006$; 9.6 days by 5 mg/kg rapamycin, $P < .004$), but all mice eventually succumbed to their tumor burden (Figure 4A), as in the wild-type mice. CRT in these immunocompromised (Rag) mice greatly increased survival time (29 days with vehicle + CRT compared to vehicle alone), and rapamycin lengthened this survival time even further (11 days by 1 mg/kg rapamycin, $P < .0003$; 22.7 days by 5 mg/kg rapamycin, $P < .00001$), but in the absence of an adaptive immune response, no mice were able to clear their tumors (Figure 4B). These findings were in support of our past findings that an immune response is necessary for clearance of this tumor type and suggest that rapamycin both enhances the effects of CRT (Rag mice), as discussed above, as well as enhances the immune-mediated clearance of HPV+ tumors (wild-type mice).

In these experiments, rapamycin was very well tolerated by the animals. Weight loss was the only significantly appreciated side effect evident in rapamycin + CRT–treated mice (data not shown), with some weight loss a common side effect of CRT alone. As low-weight animals rapidly recovered weight after completion of their treatment regimens (data not shown), rapamycin may be a relatively safe way to enhance long-term cures of HPV+ HNSCC without significantly increasing the systemic toxicities of CRT.

Rapamycin Attenuates Tumor Lactate Levels

The enhanced tumor clearance observed in wild-type mice could be related to several possible mechanisms. Our past work (in preparation), and that of others [26–29], have shown that tumor lactate production inhibits immune responses. Activated mTOR signaling promotes lactate production as a byproduct of upregulated metabolism (through GLUT1, pyruvate kinase M2, LDH, and other downstream mechanisms [18,19]), and lactate in the tumor microenvironment has been
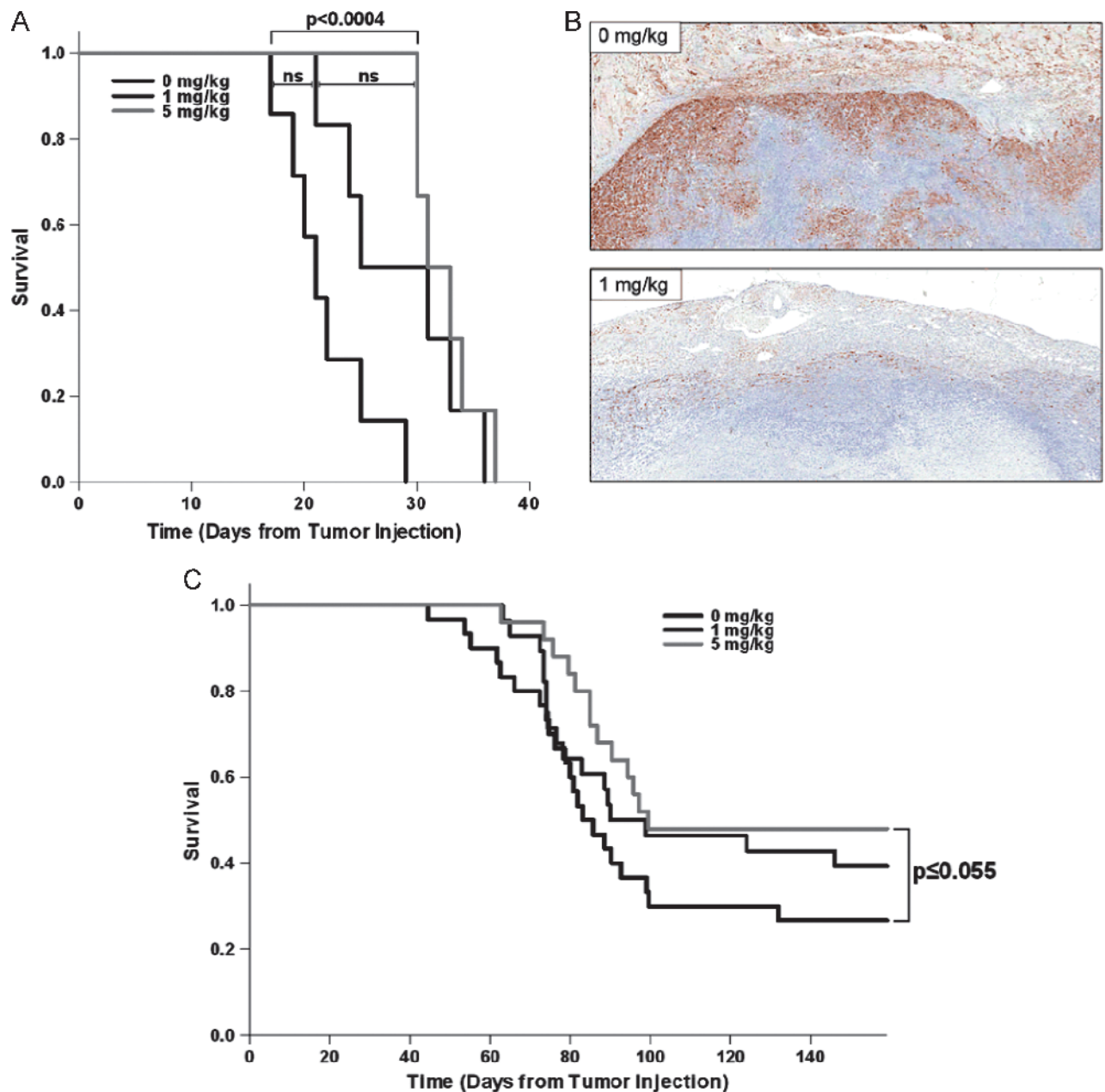
Figure 3. Rapamycin inhibits mTOR signaling at the tumor level to prolong survival and enhance CRT-induced tumor clearance in wild-type mice. (A) Kaplan-Meier survival analysis with log-rank significance test in wild-type male C57Bl/6 mice with E6/E7/Ras MOE tumors of the right flank receiving daily i.p. rapamycin or vehicle (0 mg/kg, $n = 7$; 1 mg/kg, $n = 6$; 5 mg/kg, $n = 6$; 0 to 1 mg/kg, NS; 1 to 5 mg/kg, NS; 0 to 5 mg/kg, $P < .0004$). (B) Phospho-S6 immunohistochemical staining of tumor sections harvested at end point showing inhibited mTOR signaling with rapamycin treatment (1 mg/kg). (C) Survival analysis with log-rank significance test in wild-type male C57Bl/6 mice receiving daily rapamycin or vehicle for 21 days concurrent with once weekly cisplatin (0.132 mg/mouse) and radiation (8 Gy) for 3 weeks. The combined overall survival for three separate replicates of the experiment is shown (0 mg/kg, $n = 30$; 1 mg/kg, $n = 28$; 5 mg/kg, $n = 25$; 0 to 1 mg/kg, NS; 1 to 5 mg/kg, NS; 0 to 5 mg/kg, $P \leq .055$). A rapamycin dose-dependent increase in tumor-free survival concurrent with equal dosing of CRT was observed, 27% with CRT alone, 39% at 1 mg/kg rapamycin + CRT, and 48% at 5 mg/kg rapamycin + CRT. The highest dose of rapamycin concurrent with CRT showed a 21% overall increase in tumor-free survival in wild-type mice compared to vehicle.

shown to inhibit immune cell functions [26–28], including those specific for CD8$^+$ cells [29]. Knowing HPV+ HNSCC clearance is CD8$^+$ dependent [25], we thus hypothesized that metabolic down-regulation by rapamycin could plausibly enhance the immune response necessary for HPV+ tumor clearance. Rapamycin was able to significantly diminish lactate production *in vitro* as determined by colorimetric lactate assay of culture media of both 4-hour rapamycin-treated HPV+ human (SCC47: 1 nM, $P < .01$; 10 nM, $P < .05$; 100 nM, $P <$ .02; SCC90: 10 nM, $P < .02$; 100 nM, $P < .02$) and mouse (E6/E7/Ras MOE: 10 nM, $P < .02$; 100 nM, $P < .05$) SCCs (Figure 5A). Though differing levels of lactate were reached in the 4-hour treatment time among the tested cell lines, these levels directly correlate with the intrinsic growth rates of the cell lines and thus are indicative of differing rates of lactate production rather than reflective of absolute achievable levels such as in the *in vivo* tumor microenvironment. Moreover, rapamycin significantly decreased the lactate levels in a dose-dependent

manner in all of the cell lines tested irrespective of the absolute lactate level obtained in 4 hours *in vitro*. *In vivo*, when E6/E7/Ras tumors from daily rapamycin-treated end-point mice (as described in Materials and Methods section) were sectioned and subjected to quantitative lactate bioluminescence *ex vivo* using a lactate-dependent luciferase-containing buffer system [34] (Figure 5*B*), tumor lactate levels were also seen to be significantly decreased compared to vehicle-treated mice (1 and 5 mg/kg rapamycin, $P < .0002$). Therefore, rapamycin

Figure 4. Rapamycin prolongs survival and enhances CRT in immuno-compromised mice but does not lead to any long-term cures. (A) Kaplan-Meier survival analysis with log-rank significance test in immunocompromised, Rag-1–deficient male C57Bl/6 mice with E6/E7/Ras MOE tumors receiving daily rapamycin treatment or vehicle (for all groups, $n = 5$; 0 to 1 mg/kg, $P < .006$; 1 to 5 mg/kg, NS; 0 to 5 mg/kg, $P < .004$). (B) Survival analysis with log-rank significance test in Rag-1–deficient, immunocompromised male C57Bl/6 mice receiving daily rapamycin or vehicle for 21 days concurrent with CRT as described above (0 mg/kg, $n = 10$; 1 mg/kg, $n = 9$; 5 mg/kg, $n = 9$; 0 to 1 mg/kg, $P < .0003$; 1 to 5 mg/kg, $P < .002$; 0 to 5 mg/kg, $P < .00001$).

is capable of attenuating tumor cell metabolism as indicated by reduced lactate production.

Lactic Acid Inhibits Cell-Mediated Immunity to HPV+ HNSCC

To then assess whether or not lactate is capable of attenuating HPV-related cell-mediated immunity (CMI), splenocytes isolated from HPV-16 E6/E7-vaccinated mice were co-cultured with irradiated E6/E7/Ras MOEs in known concentrations of lactic acid in media. Lactic acid was used, as lactate transport out of a cell is coupled to a proton gradient (see Discussion section below). Flow cytometry was then used to identify CFSE-stained epithelial cancer cell populations, and cell-mediated immune killing was quantified using the mean fluorescent intensity of the DNA intercalator and dead cell stain, TO-PRO-3, within the cancer cell populations. The mean fluorescent intensity of TO-PRO-3 did not significantly change in the presence of lactic acid alone [0 to 5 to 10 mM lactic acid, not significant (NS)] but was significantly increased in the presence of lymphocytes at all lactic acid concentrations ($P < .02$), indicating cell-mediated killing of the cancer cells with negligible acid effect itself. However, increasing concentrations of lactic acid significantly decreased (10 mM lactic acid, $P < .005$) the mean fluorescent intensity of TO-PRO-3 in the presence of lymphocytes (Figure 6*A*). As a possible explanation, a dose-dependent decrease in total perforin, the pore-forming protein released from CD8+ cells that allows the apoptosis-initiating granzyme B protease to enter the target cell, was observed in response to concentrations of lactic acid at 10 mM and above (Figures 6*B* and W2). These findings indicate that elevated lactate levels, as associated with upregulated metabolism, have the ability to reduce immune-mediated death of E6 and E7–expressing cancer cells.
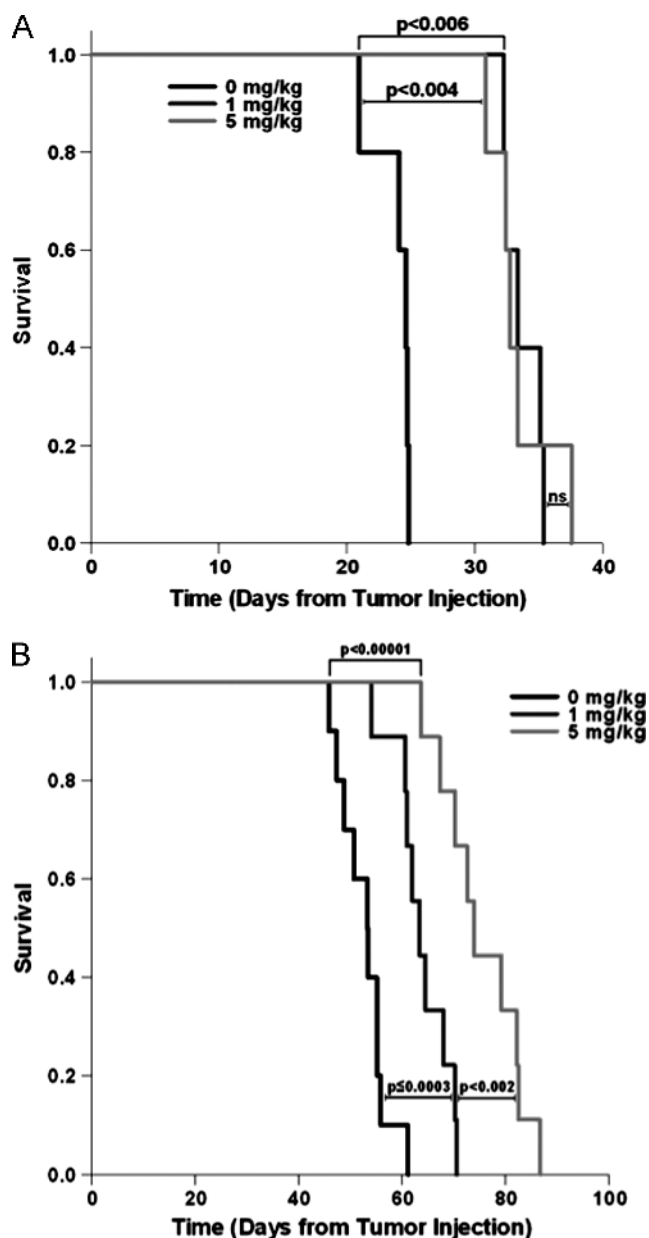
Discussion

Our recent work [9,25] has shown that successful long-term cures of HPV+ HNSCC with the current therapies of cisplatin and radiation have two mechanisms that are therapy related: 1) direct cell toxicity from both cisplatin and radiation and 2) an immune response induced during CRT. An ideal innovative drug to further improve survival in these patients would thus have three aspects: 1) it would further increase tumor-specific direct cell toxicity for CRT, 2) it would further enhance immune-related clearance that is induced by cisplatin and radiation, and 3) it would not increase systemic toxicity or morbidity. A drug that targets the viral-mediated changes of metabolism may possess these ideal characteristics for therapy. Thus, inhibiting virally enhanced mTOR signaling is likely to be a valuable therapeutic approach in HPV+ HNSCC.

mTOR inhibitors have been tested extensively in humans without severe adverse increases in systemic toxicity or morbidity. Yet, inhibiting mTOR may enhance direct toxicity to dependent HPV+ cancer cells, as suggested by our data, because the cells then lack antiapoptotic and key survival signals downstream of mTOR and cap-dependent translation, which are otherwise known to be induced by CRT [38]. In addition, past work and the data presented here suggest that reduced lactate production promotes CMI. HNSCCs have not only been shown to have high mTOR activity [39] but have also been shown to overexpress downstream metabolic enzymes including LDH [40], an indicator of poor prognosis. Targeting of mTOR downregulates these enzymes and impedes growth signaling, attenuating metabolism and, subsequently, lactate production. Lactate is transported from a
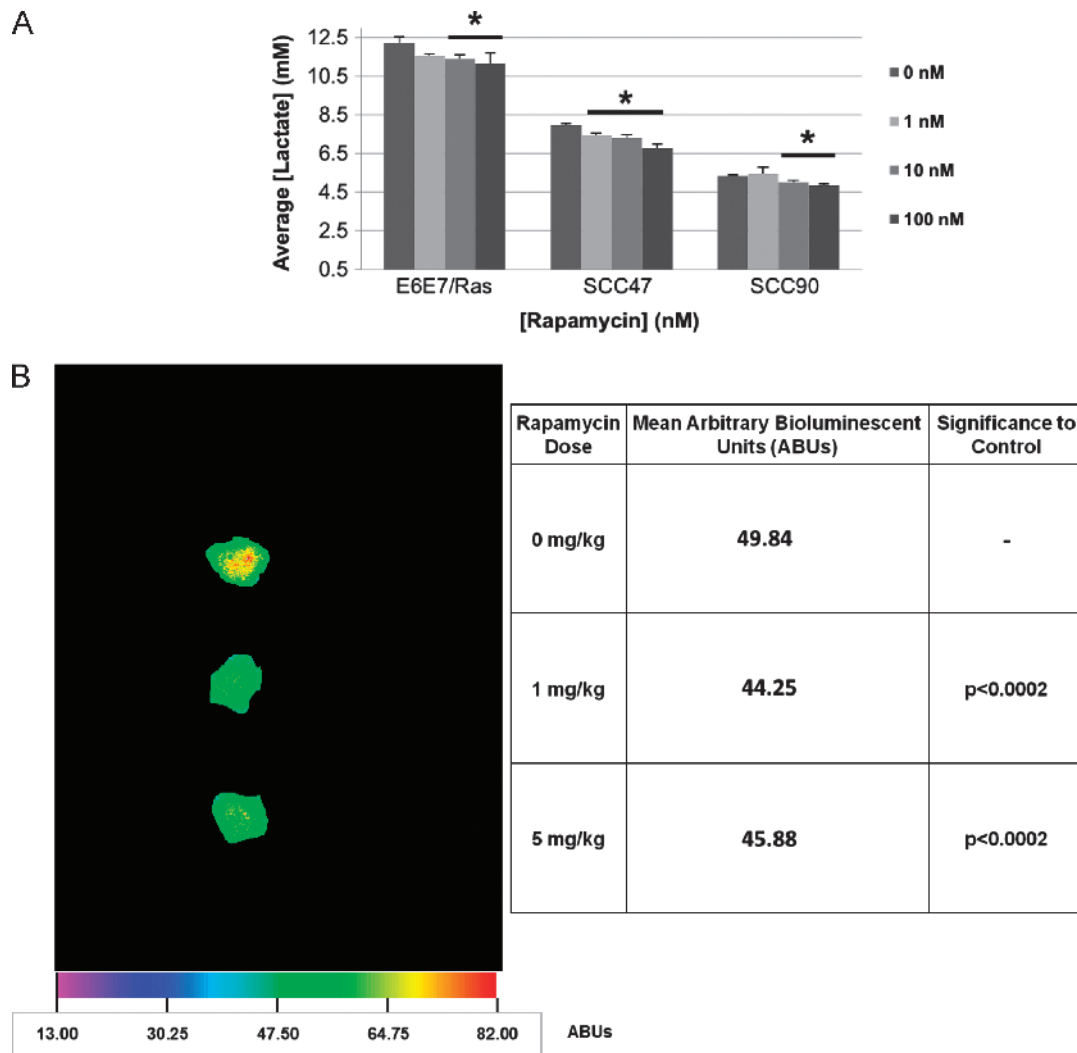
Figure 5. Rapamycin attenuates tumor cell lactate production. (A) *In vitro* lactate assay. E6/E7/Ras MOEs or HPV+ SCCs plated to 100% confluence were incubated for 4 hours in the presence of the indicated doses of rapamycin. The media was then subject to a commercially available colorimetric lactate assay, the concentration determined through standard curve, and the results plotted as average lactate concentration per dosage group ($n = 3$). Rapamycin significantly decreased lactate production in both HPV+ SCC (SCC47: 1 nM, $P < .01$; 10 nM, $P < .05$; 100 nM, $P < .02$; SCC90: 10 nM, $P < .02$; 100 nM, $P < .02$) and E6/E7/Ras MOE (10 nM, $P < .02$; 100 nM, $P < .05$) cell lines. (B) Quantitative lactate bioluminescence. Lactate levels were visualized in end-point tumor sections of E6/E7/Ras tumors from daily vehicle or rapamycin-treated C57Bl/6 mice using a lactate-dependent luciferase-containing buffer system as described by Broggini-Tenzer et al. [34]. Intensities of bioluminescent images of six ($n = 6$) tumor sections from multiple mice at each dosage group were averaged. A representative image is shown alongside tabulated mean bioluminescent intensity and P values compared to control per dosage group (1 to 5 mg/kg, NS).

cell with a proton in the form of lactic acid and has been suggested to reach concentrations of up to 40 mM in the microenvironment of solid tumors and 20 mM in cell culture ([29] and references therein). Indeed, concentrations upward of 10 mM are feasible also on the basis of our data. These high lactate concentrations can affect the cytotoxic activity of CD8+ lymphocytes, which is supported by our findings. This appears to be specific to lactic acid and not a general acid effect, as demonstrated by Fischer et al. when comparing the inhibition of cytotoxic T-lymphocytes by lactic to that by hydrochloric acid [29]. This is explained at least in part through abolishment of lactate/proton co-transport down their concentration gradient into the extracellular space. Intracellular accumulation of lactate ultimately culminates in a metabolic blockade, reducing the translation and subsequent availability of intracellular perforin, the primer of cell-mediated cytotoxicity, among other proteins [29]. mTOR inhibition thus plausibly enhances

immune-related tumor clearance, as induced by CRT and seen in our animal studies.

This is not to say that other players in the tumor microenvironment do not affect immune and therapeutic responses in other ways but highlights a likely contributing factor and the importance of understanding the role of the tumor microenvironment. In addition to effects on other immune cell functions [26–29], elevated tumor lactate levels have been associated with radioresistance [41], enhanced malignant behavior through up-regulation of vascular endothelial growth factor and HIF1α, and enhanced cellular motility [42]. Local acidification associated with lactate also has positive effects on matrix degradation, and lactate has been shown to induce other factors important for tumor progression such as CD44, hyaluronic acid, and transforming growth factor–β [43]. Lactate has also been suggested to play a role in symbiotic cancer-stromal interactions, whereby a tumor favorable

microenvironment is created, reciprocal metabolites are provided, and metabolic reprogramming is induced under control of the downstream target of mTOR, HIF1α [44]. Taken together with its control over the metabolic enzymes of lactate production, our results suggest that mTOR represents a strong candidate therapeutic target for immunogenic, HPV-related cancers, which exhibit elevated mTOR function [14,39], and that mTOR inhibition logically accents standard-of-care CRT for HPV+ HNSCC.

Though HPV– HNSCCs are known to commonly harbor activating mutations in the mTOR signaling pathway [15,35], our studies focused on hypotheses of improving tumor clearance through mechanisms of enhanced immune response. The HPV– cell lines tested in this work did show mTOR and growth inhibition with rapamycin treatment. Thus, HPV– cancers, or any showing some mTOR dependence, may be susceptible to the enhanced direct cell killing of the CRT/rapamycin combination suggested by our *in vitro* and Rag mouse studies. Yet, the role of the immune system regarding HPV– cancers is less well understood. It is likely that other non-HPV tumor antigens are present and aid in clearance in at least a subset of HPV– cancers because immunosuppressed patients respond worse to treatment.
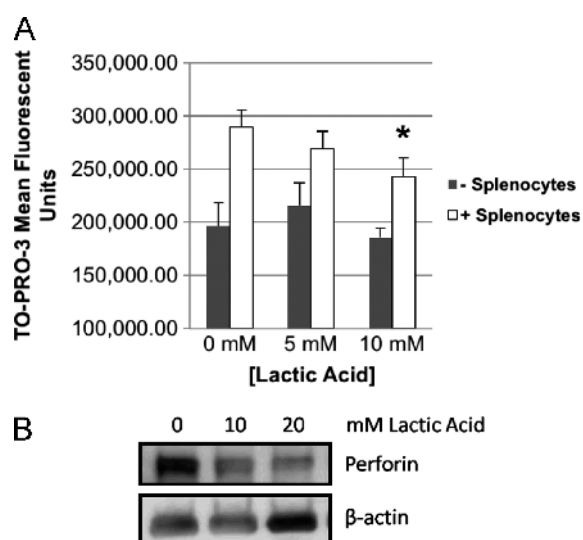

Figure 6. Lactic acid inhibits CMI and decreases lymphocyte perforin levels specific to our HPV+ HNSCC tumor model. (A) CMI assay. CFSE-stained E6/E7/Ras cells were irradiated (30 Gy) and co-cultured for 24 hours with isolated mixed lymphocytes from the spleens of mice vaccinated with Ad5 E6/E7 [6] at 0, 5, and 10 mM lactic acid in media (RPMI) followed by dead cell staining (TO-PRO-3) and flow cytometry. CFSE-positive cells were gated and mean TO-PRO-3 signal averaged ($n = 3$) for each dosage group. In all dosage groups, the presence of lymphocytes led to significantly increased dead cell staining ($P < .02$), while lactic acid in the absence of lymphocytes did not itself induce any cell death (splenocytes: 0, 5, and 10 mM, NS). A trend of decreasing dead cell staining with increasing lactic acid concentration was observed. At 10 mM lactic acid, cell-mediated cytotoxicity was significantly decreased as indicated by decreased dead cell staining (*$P < .005$). (B) Lymphocytes cultured alone in lactic acid for 24 hours showed a dose-dependent decrease by Western blot in total perforin, the primer of CMI. Concentrations of lactic acid at 10 mM and higher were tested as significant inhibition of CMI was not seen at less than 10 mM. The blot has been cropped for presentation and can be seen in full in Figure W2.

Inhibition of mTOR has been shown to be promising therapeutically for HPV– HNSCCs ([39] and references therein), which is preliminarily supported by our *in vitro* findings, but further work is necessitated to evaluate mTOR inhibition concurrent to CRT for HPV– HNSCC in light of the immune system. Fortunately, there are a number of clinical trials of mTOR inhibitors combined with various treatment modalities for HNSCC underway [45], which should help to address this uncertainty of the HPV– cancers, but careful retrospective analysis will be necessary as the improved treatment response of HPV+ HNSCCs can be confounding as a cancer type now recognized as a distinct clinical entity.

In addition to the known, and likely contributory, suppressive effects on cancer cell proliferation and angiogenesis, mTOR inhibition may also enhance CRT of HPV+ HNSCC beyond impeded survival signals and disinhibition of immune cell function through some yet to be fully elucidated combinatorial sensitizing mechanism, such as enhancement of immunogenic cell death. Signaling through mTOR normally inhibits autophagy, which can act as an immunogenic form of cell death. mTOR inhibition has been shown to enhance autophagy [46], which is also induced by CRT [47,48], thus providing a possible explanation for the enhancement of both direct CRT-induced cytotoxicity and immune-mediated tumor clearance suggested by this work. Furthermore, inhibitors of mTOR, through stimulation of autophagy, have been shown to synergize with cisplatin in the killing of oropharyngeal carcinoma [49]. However, the specific cell death mechanism is important as autophagy can also be cytoprotective [50] and not all forms of cell death are immunogenic [51]. Future work is necessary for identification of the predominant cell death mechanism induced by the rapamycin/CRT combination.

Of interest, our results also suggest that mTOR inhibition by rapamycin with and without the combination of standard-of-care CRT may also be of benefit to immunocompromised HPV+ cancer patients, such as patients with human immunodeficiency virus/acquired immunodeficiency syndrome (HIV/AIDS) who have an inherently increased risk of HPV infection and associated cancers [52,53]. Though our data suggests that an intact immune system is necessary for tumor clearance, significantly prolonged tumor-bearing survival was observed in immunocompromised animals receiving rapamycin with and without CRT. It is therefore possible that rapamycin may prolong survival and potentially enhance tumor clearance even when immune response is weakened by HIV or in other immunosuppressive conditions. In addition to HIV patients, high-risk HPV infection and increased risk of subsequent carcinogenesis has been associated with many states of chronic immune suppression, such as after renal transplant (an instance when rapamycin is commonly prescribed in an immunosuppressant combination to prevent organ rejection) and with autoimmune diseases [54,55], making our findings potentially widely applicable.

This work adds to the knowledge of virally related metabolic changes and may help to translate that knowledge into newer, safer therapies that can augment the current standard-of-care treatment of HPV+ HNSCC. mTOR is one such therapeutic target that may prove to be effectively inhibited concurrent with standard-of-care platinum-based chemotherapy and radiation, enhancing direct cytotoxicity and inhibiting tumor growth and lactate production to allow for a more effective immune response to this antigenic tumor type without increasing systemic toxicities. These findings may have broad implications for many solid cancers showing mTOR dependence and that are treated with chemoradiation, particularly those expressing viral antigens, and may impact their clinical management.

Acknowledgments

References

[1] American Cancer Society (2011). *Cancer Facts & Figures 2011.* American Cancer Society, Atlanta, GA.

[2] Marklund L and Hammarstedt L (2011). Impact of HPV in oropharyngeal cancer. *J Oncol* **2011**, 509036.

[3] Dufour X, Beby-Defaux A, Agius G, and Lacau St Guily J (2012). HPV and head and neck cancer. *Eur Ann Otorhinolaryngol Head Neck Dis* **129**, 26–31.

[4] Gillison M, Kahle L, Graubard BI, and Chaturvedi AK (2012). Prevalence of oral HPV infection in the United States, 2009–2010. *JAMA* **307**, 699–703.

[5] Marur S, D'Souza G, Westra WH, and Forastiere A (2010). HPV-associated head and neck cancer: a virus-related cancer epidemic. *Lancet Oncol* **11**, 781–789.

[6] Lee DW, Anderson ME, Wu S, and Lee JH (2008). Development of an adenoviral vaccine against E6 and E7 oncoproteins to prevent growth of human papillomavirus-positive cancer. *Arch Otolaryngol Head Neck Surg* **134**, 1316–1323.

[7] Hoover AC, Spanos WC, Harris GF, Mary E, Klingelhutz AJ, and Lee JH (2007). The role of human papillomavirus 16 E6 in anchorage-independent and invasive growth of mouse tonsil epithelium. *Arch Otolaryngol Head Neck Surg* **133**, 495–502.

[8] Schlecht NF, Burk RD, Adrien L, Dunne A, Kawachi N, Sarta C, Chen Q, Brandwein-Gensler M, Prystowsky MB, Childs G, et al. (2007). Gene expression profiles in HPV-infected head and neck cancer. *J Pathol* **213**, 283–293.

[9] Spanos WC, Nowicki P, Lee DW, Hoover A, Hostager B, Gupta A, Anderson ME, and Lee JH (2009). Immune response during therapy with cisplatin or radiation for human papillomavirus-related head and neck cancer. *Arch Otolaryngol Head Neck Surg* **135**, 1137–1146.

[10] Mazurek S (2011). Pyruvate kinase type M2: a key regulator of the metabolic budget system in tumor cells. *Int J Biochem Cell Biol* **43**, 969–980.

[11] Mazurek S, Zwerschke W, Jansen-Durr P, and Eigenbrodt E (2001). Effects of the human papilloma virus HPV-16 E7 oncoprotein on glycolysis and glutaminolysis: role of pyruvate kinase type M2 and the glycolytic-enzyme complex. *Biochem J* **356**, 247–256.

[12] Leemans CR, Braakhuis BJM, and Brakenhoff RH (2011). The molecular biology of head and neck cancer. *Nat Rev Cancer* **11**, 9–22.

[13] Noch E and Khalili K (2012). Oncogenic viruses and tumor glucose metabolism: like kids in a candy store. *Mol Cancer Ther* **11**, 14–23.

[14] Spangle JM and Münger K (2010). The human papillomavirus type 16 E6 oncoprotein activates mTORC1 signaling and increases protein synthesis. *J Virol* **84**, 9398–9407.

[15] Liao Y-M, Kim C, and Yen Y (2011). Mammalian target of rapamycin and head and neck squamous cell carcinoma. *Head Neck Oncol* **3**, 22.

[16] Hu M, Ekshyyan O, Herman Ferdinandez L, Rong X, Caldito G, and Nathan C-AO (2011). Efficacy and comparative effectiveness of sirolimus as an anticancer drug. *Laryngoscope* **121**, 978–982.

[17] Molinolo A, Hewitt SM, Amornphimoltham P, Keelawat S, Rangdaeng S, Meneses García A, Raimondi AR, Jufe R, Itoiz M, Gao Y, et al. (2007). Dissecting the Akt/mammalian target of rapamycin signaling network: emerging results from the head and neck cancer tissue array initiative. *Clin Cancer Res* **13**, 4964–4973.

[18] Tennant DA (2011). PK-M2 makes cells sweeter on HIF1. *Cell* **145**, 647–649.

[19] Luo W and Semenza GL (2011). Pyruvate kinase M2 regulates glucose metabolism by functioning as a coactivator for hypoxia-inducible factor 1 in cancer cells. *Oncotarget* **2**, 551–556.

[20] Amornphimoltham P, Leelahavanichkul K, Molinolo A, Patel V, and Gutkind JS (2008). Inhibition of mammalian target of rapamycin by rapamycin causes the regression of carcinogen-induced skin tumor lesions. *Clin Cancer Res* **14**, 8094–8101.

[21] Raimondi AR, Molinolo A, and Gutkind JS (2009). Rapamycin prevents early onset of tumorigenesis in an oral-specific K-ras and p53 two-hit carcinogenesis model. *Cancer Res* **69**, 4159–4166.

[22] Czerninski R, Amornphimoltham P, Patel V, Molinolo A, and Gutkind JS (2009). Targeting mammalian target of rapamycin by rapamycin prevents tumor progression in an oral-specific chemical carcinogenesis model. *Cancer Prev Res (Phila)* **2**, 27–36.

[23] Amornphimoltham P, Patel V, Leelahavanichkul K, Abraham RT, and Gutkind JS (2008). A retroinhibition approach reveals a tumor cell–autonomous response to rapamycin in head and neck cancer. *Cancer Res* **68**, 1144–1153.

[24] Patel V, Marsh CA, Dorsam RT, Mikelis CM, Masedunskas A, Amornphimoltham P, Nathan CA, Singh B, Weigert R, Molinolo AA, et al. (2011). Decreased lymphangiogenesis and lymph node metastasis by mTOR inhibition in head and neck cancer. *Cancer Res* **71**, 7103–7112.

[25] Williams R, Lee DW, Elzey BD, Anderson ME, Hostager BS, and Lee JH (2009). Preclinical models of HPV+ and HPV– HNSCC in mice: an immune clearance of HPV+ HNSCC. *Head Neck* **31**, 911–918.

[26] Gottfried E, Kunz-Schughart LA, Ebner S, Mueller-Klieser W, Hoves S, Andreesen R, Mackensen A, and Kreutz M (2006). Tumor-derived lactic acid modulates dendritic cell activation and antigen expression. *Blood* **107**, 2013–2021.

[27] Shime H, Yabu M, Akazawa T, Kodama K, Matsumoto M, Seya T, and Inoue N (2008). Tumor-secreted lactic acid promotes IL-23/IL-17 proinflammatory pathway. *J Immunol* **180**, 7175–7183.

[28] Goetze K, Walenta S, Ksiazkiewicz M, Kunz-Schughart LA, and Mueller-Klieser W (2011). Lactate enhances motility of tumor cells and inhibits monocyte migration and cytokine release. *Int J Oncol* **39**, 453–463.

[29] Fischer K, Hoffmann P, Voelkl S, Meidenbauer N, Ammer J, Edinger M, Gottfried E, Schwarz S, Rothe G, Hoves S, et al. (2007). Inhibitory effect of tumor cell-derived lactic acid on human T cells. *Blood* **109**, 3812–3819.

[30] Amiel E, Everts B, Freitas TC, King IL, Curtis JD, Pearce EL, and Pearce EJ (2012). Inhibition of mechanistic target of rapamycin promotes dendritic cell activation and enhances therapeutic autologous vaccination in mice. *J Immunol* **189**, 2151–2158.

[31] Srivastava RK, Utley A, and Shrikant PA (2012). Rapamycin: a rheostat for CD8+ T-cell-mediated tumor therapy. *Oncoimmunology* **1**, 1189–1190.

[32] Hoover AC, Strand GL, Nowicki PN, Anderson ME, Vermeer PD, Klingelhutz AJ, Bossler AD, Pottala JV, Hendriks W, and Lee JH (2009). Impaired PTPN13 phosphatase activity in spontaneous or HPV-induced squamous cell carcinomas potentiates oncogene signaling through the MAP kinase pathway. *Oncogene* **28**, 3960–3970.

[33] Brenner JC, Graham MP, Kumar B, Lindsay M, Kupfer R, Lyons RH, Bradford CR, and Carey TE (2010). Genotyping of 73 UM-SCC head and neck squamous cell carcinoma cell lines. *Head Neck* **32**, 417–426.

[34] Broggini-Tenzer A, Vuong V, and Pruschy M (2011). Metabolism of tumors under treatment: mapping of metabolites with quantitative bioluminescence. *Radiother Oncol* **99**, 398–403.

[35] Amornphimoltham P, Patel V, Sodhi A, Nikitakis NG, Sauk JJ, Sausville EA, Molinolo AA, and Gutkind JS (2005). Mammalian target of rapamycin, a molecular target in squamous cell carcinomas of the head and neck. *Cancer Res* **65**, 9953–9961.

[36] Iglesias-Bartolome R, Patel V, Cotrim A, Leelahavanichkul K, Molinolo A, Mitchell JB, and Gutkind JS (2012). mTOR inhibition prevents epithelial stem cell senescence and protects from radiation-induced mucositis. *Cell Stem Cell* **11**, 401–414.

[37] Lill C, Kornek G, Bachtiary B, Selzer E, Schopper C, Mittlboeck M, Burian M, Wrba F, and Thurnher D (2011). Survival of patients with HPV-positive oropharyngeal cancer after radiochemotherapy is significantly enhanced. *Wien Klin Wochenschr* **123**, 215–221.

[38] Ekshyyan O, Rong Y, Rong X, Pattani KM, Abreo F, Caldito G, Kai Siung Chang J, Ampil F, Glass J, and Nathan C-AO (2009). Comparison of radiosensitizing effects of the mammalian target of rapamycin inhibitor CCI-779 to cisplatin in experimental models of head and neck squamous cell carcinoma. *Mol Cancer Ther* **8**, 2255–2265.

[39] Molinolo A, Marsh C, El Dinali M, Gangane N, Jennison K, Hewitt SM, Patel V, Seiwert TY, and Gutkind JS (2012). mTOR as a molecular target in HPV-associated oral and cervical squamous carcinomas. *Clin Cancer Res* **18**, 2558–2568.

[40] Koukourakis MI, Giatromanolaki A, Winter S, Leek R, Sivridis E, and Harris AL (2009). Lactate dehydrogenase 5 expression in squamous cell head and neck cancer relates to prognosis following radical or postoperative radiotherapy. *Oncology* **77**, 285–292.

[41] Quennet V, Yaromina A, Zips D, Rosner A, Walenta S, Baumann M, and Mueller-Klieser W (2006). Tumor lactate content predicts for response to fractionated irradiation of human squamous cell carcinomas in nude mice. *Radiother Oncol* **81**, 130–135.

[42] Walenta S, Schroeder T, and Mueller-Klieser W (2004). Lactate in solid malignant tumors: potential basis of a metabolic classification in clinical oncology. *Curr Med Chem* **11**, 2195–2204.

[43] Gottfried E, Kreutz M, and Mackensen A (2012). Tumor metabolism as modulator of immune response and tumor progression. *Semin Cancer Biol* **22**, 335–341.

[44] Fiaschi T, Marini A, Giannoni E, Taddei ML, Gandellini P, De Donatis A, Lanciotti M, Serni S, Cirri P, and Chiarugi P (2012). Reciprocal metabolic reprogramming through lactate shuttle coordinately influences tumor-stroma interplay. *Cancer Res* **72**, 5130–5140.

[45] Gao W, Zeng J, Li H, Yu J, Chan W, Ho WK, and Wong T-S (2012). mTOR pathway and mTOR inhibitors in head and neck cancer. *Otolaryngology* **2012**, 1–7.

[46] Iwamaru A, Kondo Y, Iwado E, Aoki H, Fujiwara K, Yokoyama T, Mills GB, and Kondo S (2007). Silencing mammalian target of rapamycin signaling by small interfering RNA enhances rapamycin-induced autophagy in malignant glioma cells. *Oncogene* **26**, 1840–1851.

[47] Kim KW, Hwang M, Moretti L, Jaboin JJ, Cha YI, and Lu B (2008). Autophagy upregulation by inhibitors of caspase-3 and mTOR enhances radiotherapy in a mouse model of lung cancer. *Autophagy* **4**, 659–668.

[48] Cao C, Subhawong T, Albert JM, Kim KW, Geng L, Sekhar KR, Gi YJ, and Lu B (2006). Inhibition of mammalian target of rapamycin or apoptotic pathway induces autophagy and radiosensitizes PTEN null prostate cancer cells. *Cancer Res* **66**, 10040–10047.

[49] Galluzzi L, Senovilla L, Vitale I, Michels J, Martins I, Kepp O, Castedo M, and Kroemer G (2011). Molecular mechanisms of cisplatin resistance. *Oncogene* **31**, 1869–1883.

[50] Ren J-H, He W-S, Nong L, Zhu Q-Y, Hu K, Zhang R-G, Huang L-L, Zhu F, and Wu G (2010). Acquired cisplatin resistance in human lung adenocarcinoma cells is associated with enhanced autophagy. *Cancer Biother Radiopharm* **25**, 75–80.

[51] Tesniere A, Apetoh L, Ghiringhelli F, Joza N, Panaretakis T, Kepp O, Schlemmer F, Zitvogel L, and Kroemer G (2008). Immunogenic cancer cell death: a key-lock paradigm. *Curr Opin Immunol* **20**, 504–511.

[52] Frisch M, Biggar RJ, and Goedert JJ (2000). Human papillomavirus-associated cancers in patients with human immunodeficiency virus infection and acquired immunodeficiency syndrome. *J Natl Cancer Inst* **92**, 1500–1510.

[53] Chaturvedi AK, Madeleine MM, Biggar RJ, and Engels E (2009). Risk of human papillomavirus-associated cancers among persons with AIDS. *J Natl Cancer Inst* **101**, 1120–1130.

[54] Hinten F, Meeuwis KAP, Van Rossum MM, and De Hullu JA (2012). HPV-related (pre)malignancies of the female anogenital tract in renal transplant recipients. *Crit Rev Oncol Hematol* **84**, 161–180.

[55] Aubin F, Martin M, Puzenat E, Magy-Bertrand N, Segondy M, Riethmuller D, and Wendling D (2011). Genital human papillomavirus infection in patients with autoimmune inflammatory diseases. *Joint Bone Spine* **78**, 460–465.
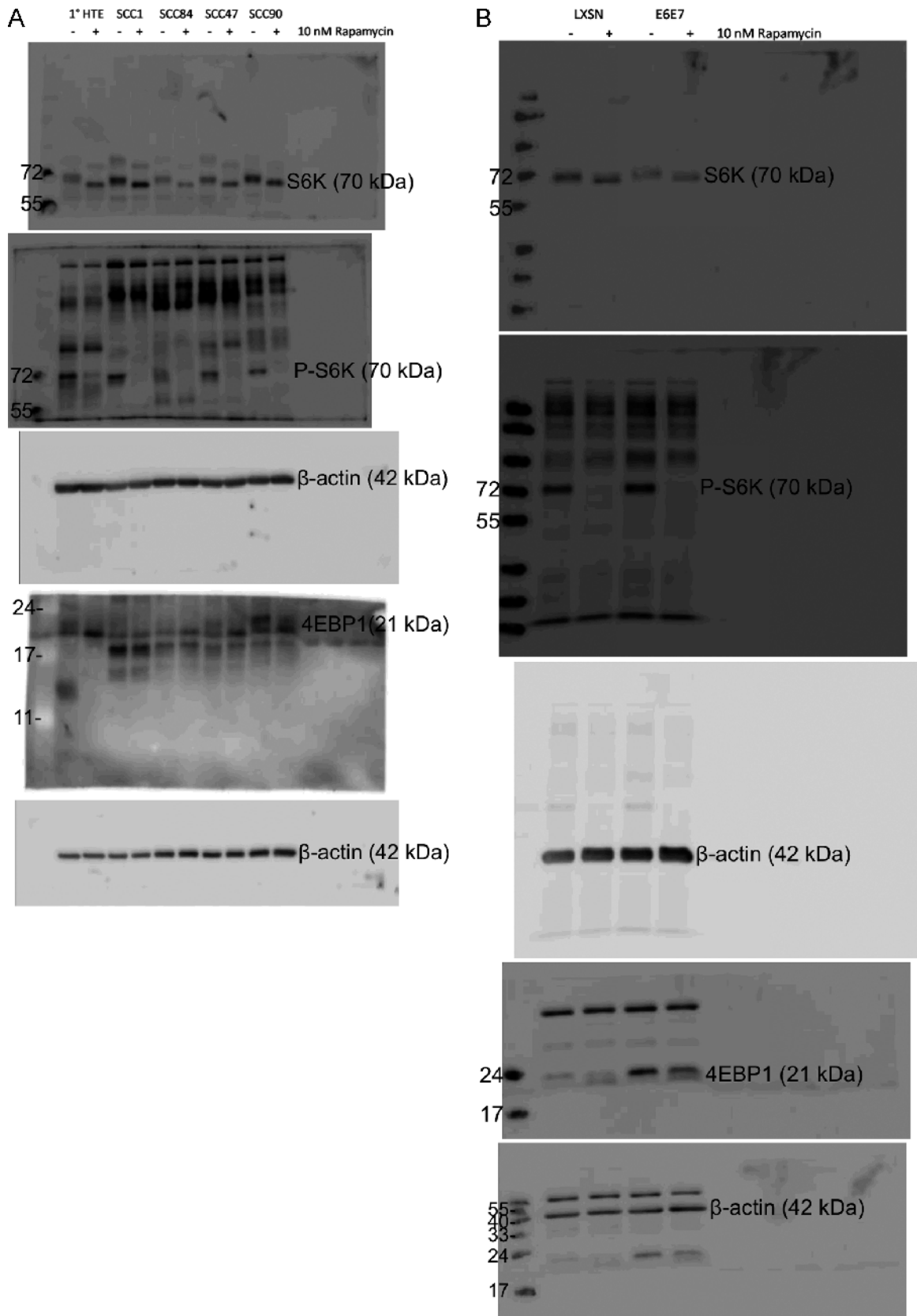
Figure W1. Full-length Western blots with size markers of downstream targets of mTOR corresponding to those shown in Figure 1 of the main text. Blots for P-S6K, total S6K, and 4EBP1 are shown. β-Actin is shown as a loading control. (A) Primary HTEs are compared to four tonsillar SCC lines, two HPV− (SCC1 and SCC84) and two HPV+ (SCC47 and SCC90), after 24 hours of treatment with 10 nM rapamycin or vehicle. (B) A retrovirally transduced and immortalized HPV+ mouse oropharyngeal epithelial (MOE) cell line possessing the E6 and E7 oncogenes (E6/E7) is compared to an empty vector containing control line (LXSN).
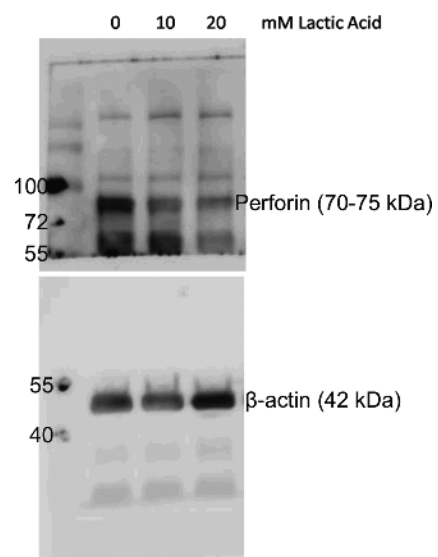
Figure W2. Full-length Western blot with size markers of mouse perforin corresponding to the blot shown in Figure 6 of the main text. β-Actin is shown as a loading control. Perforin was blotted from whole-cell lysates of mixed lymphocytes that were cultured for 24 hours at 0, 10, and 20 mM lactic acid in media (RPMI), which were isolated from the spleens of mice vaccinated with Ad5 E6/E7.